

## Electronic Supplementary Information (ESI)

### The self-assembly and metal adatom coordination of a linear bis-tetrazole ligand on Ag(111)

Peter Knecht<sup>1</sup>, Nithin Suryadevara<sup>2</sup>, Bodong Zhang<sup>1</sup>, Joachim Reichert<sup>1</sup>, Mario Ruben<sup>2,3</sup>, Johannes V. Barth<sup>1</sup>, Svetlana Klyatskaya<sup>2</sup>, and Anthoula C. Papageorgiou<sup>1</sup>

<sup>1</sup>Physics Department E20, Technical University of Munich, D-85748 Garching, Germany

<sup>2</sup>Institute of Nanotechnology, Karlsruhe Institute of Technology, D-76344 Eggenstein-Leopoldshafen, Germany

<sup>3</sup>Institute de Physique et Chimie de Matériaux (IPCMS), CNRS-Université Strasbourg, 23 rue du Loess, BP 43, F-67034 Strasbourg Cedex 2, France

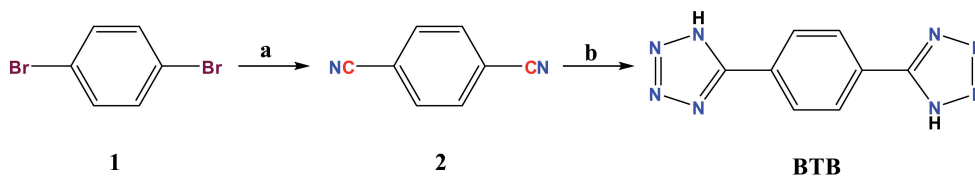
### Contents

Experimental procedures . . . . .	S-2
Scheme S1: BTB synthesis . . . . .	S-2
Figure S1: View of BTB crystal structure . . . . .	S-4
Figure S2: Model of phase $\alpha$ with <i>cis</i> isomers . . . . .	S-4
Figure S3: C 1s and N 1s spectra of BTB on Ag(111) evolving with time . . . . .	S-5
Table S1: Relative intensities of XPS peaks . . . . .	S-5
Table S2: Atomic ratios of C, N, and Fe . . . . .	S-6
Figure S4: STM image of phases $\beta$ and $\gamma$ with visible Ag adatoms . . . . .	S-6
Figure S5: Illustration of the chiral recognition in the boundaries of phases $\beta$ and $\gamma$ . . . . .	S-6
Figure S6: Chirality switch in phase $\delta$ . . . . .	S-7
Figure S7: STM images of phases $\delta$ and $\epsilon$ with visible Fe adatoms . . . . .	S-7
Figure S8: Overview of polymorphism . . . . .	S-8

## Experimental procedures

### Synthesis:

**General:** All the starting materials were purchased from commercial sources and were used as received. Solvents were freshly distilled over appropriate drying reagents.  $^1\text{H}$  and  $^{13}\text{C}$  NMR measurements were recorded using a Bruker Ultrashield plus 500 spectrometer with solvent-proton as an internal standard. Elemental analyses were carried out on a Vario Micro Cube. Infrared spectra were recorded using KBr-pressed pellets with a Perkin-Elmer Spectrum GX FT-IR spectrometer in the region of  $4000 - 400\text{ cm}^{-1}$ . Mass spectrometric data were acquired with a MicroTOF-Q II Bruker for ESI-TOF.



Scheme S1: Synthesis of ligand BTB, (a) CuCN, DMF, reflux, 24 h (b)  $\text{NaN}_3$ ,  $\text{NH}_4\text{Cl}$ , DMF, 400 K, 2 h.

**Procedure:** The molecule BTB was synthesized from dibromobenzene in two steps with dicyanobenzene as an intermediate molecule (Scheme S1).

### Synthesis of Dicyanobenzene (2):

Compound 2 was synthesized by means of substitution reaction with Cuprous Cyanide (CuCN) on dibromobenzene following the procedure similar to literature.<sup>1,2</sup> CuCN (3.44 g, 38.42 mmol, 3 eq) was dried under vacuum for 3 hours. Then, the copper salt and dibromobenzene (1) (3.03 g, 12.82 mmol, 1 eq) were suspended in dry DMF (60 mL), and the mixture was stirred at reflux temperature for 24 h. After cooling to room temperature, ammonium hydroxide ( $\text{NH}_4\text{OH}$ ) was added and stirred at 340 K for 2 hours. The dark blue reaction mixture was extracted with  $\text{CH}_2\text{Cl}_2$ . The organic phase was washed with brine and water, dried over anhydrous  $\text{Na}_2\text{SO}_4$  and evaporated under reduced pressure. The product was obtained by column chromatography on silica as stationary phase a gradient of  $\text{CH}_2\text{Cl}_2$  and n-hexane as a liquid phase to yield colourless product 2 (1.15 g, yield: 70 %).

$^1\text{H}$  NMR (500 MHz,  $\text{CDCl}_3$ ):  $\delta = 7.82$  (s)ppm.

$^{13}\text{C}$  NMR (126 MHz,  $\text{CDCl}_3$ ):  $\delta = 132.81, 117.01, 116.75$  ppm.

**Elemental Analysis:** Calculated (%) for  $\text{C}_8\text{H}_6\text{N}_2$ : C 75.00, H 3.15, N 21.85; found (%): C 74.76, H 3.13, N 21.63.

**FT-IR** (KBr):  $\tilde{\nu} = 3398, 3098, 3052, 2999, 2819, 2232, 1942, 1811, 1690, 1503, 1402, 1278, 1193, 1026, 845, 641, 561\text{ cm}^{-1}$ .

### Synthesis of BTB:

BTB was synthesized using microwave radiation according to the literature.<sup>3</sup> 2 (200 mg, 1.66 mmol, 1 eq), Sodium azide ( $\text{NaN}_3$ ) (610 mg, 9.36 mmol, 6 eq), and ammonium chloride ( $\text{NH}_4\text{Cl}$ ) (500 mg, 9.36 mmol, 6 eq) and dry DMF (10 mL) were added into a microwave vessel, which was then capped. The microwave vessel was then placed in a microwave reactor. The reaction was magnetically stirred and heated for 2 h at 400 K. The mixture was cooled to room temperature and then acidified with 1 M HCl solution to pH of 2. The precipitate formed was filtered by washing with water and dried to yield

colourless product BTB (320 mg, yield: 90 %).

$^1\text{H NMR}$  (500 MHz,  $(\text{CD}_3)_2\text{SO}$ ):  $\delta = 8.55$  (s)ppm.

$^{13}\text{C NMR}$  (126 MHz,  $\text{CDCl}_3$ ):  $\delta = 128.38, 127.17$  ppm.

ES-MS (in DMSO):  $m/z = 213.0534$  ( $[\text{M-H}]^- = [\text{C}_8\text{H}_6\text{N}_8\text{-H}]^- = 213.0632$ )

**Elemental Analysis:** Calculated (%) for  $\text{C}_8\text{H}_4\text{N}_8$ : C 44.90, H 2.80, N 52.30; found (%): C 44.82, H 2.81, N 51.80.

FT-IR (KBr):  $\tilde{\nu} = 3438, 3142, 3065, 3013, 2967, 2931, 2847, 2693, 2617, 2561, 2466, 2127, 1895, 1585, 1504, 1491, 1456, 1405, 1281, 1252, 1177, 1131, 1109, 1804, 1054, 1030, 991, 853, 733, 706, 530, 479, 437$   $\text{cm}^{-1}$ .

**Sample preparation:** Samples were prepared in two different ultra-high vacuum (UHV) systems with base pressures  $\sim 2 \times 10^{-10}$  mbar following similar procedures. The atomically flat Ag(111) single crystal surface (Surface Preparation laboratory, polished to  $\sim 0.1^\circ$ ) was prepared by multiple cycles of  $\text{Ar}^+$  sputtering (1 kV, 15 min) and subsequent annealing (630 K, 20 min). The BTB molecules were dosed by organic molecular beam epitaxy (OMBE) on Ag(111) surfaces held at room temperature (RT) following thorough outgassing in vacuo. The sublimation temperature was 523 K and resulted in a rate of  $\sim 0.03$  monolayers per min. One monolayer corresponds to the density of BTB in phase  $\alpha$ . A commercial OMBE source (DODECON nanotechnology GmbH) was used for the samples prepared for scanning tunneling microscopy (STM) characterisation, whereas a home built source was employed for the samples prepared for X-ray photoelectron spectroscopy (XPS) measurements.

**STM:** Measurements were performed by using an Aarhus-type STM (SPECS GmbH) operated at room temperature with chemically etched tungsten tips. The STM was operated in constant current mode and the tunnelling bias was applied to the sample.

**XPS:** Spectra were recorded with a SPECS Phoibos 150 hemispherical analyser in a SPECS GmbH UHV system at the Technical University of Munich - Walter Schottky Institute laboratory. The Mg  $\text{K}_\alpha$  line ( $h\nu = 1253.6$  eV) of a SPECS FR 50 was used as radiation source. Experiments were performed in normal emission mode, the binding energy scales of the spectra were calibrated by the Ag  $3d_{5/2}$  line at 368.2 eV. For the C 1s peaks, a Shirley background was subtracted, for the N 1s and Fe  $2p_{3/2}$  peaks polynomial backgrounds were subtracted due to the overlap with peaks from the Ag substrate.

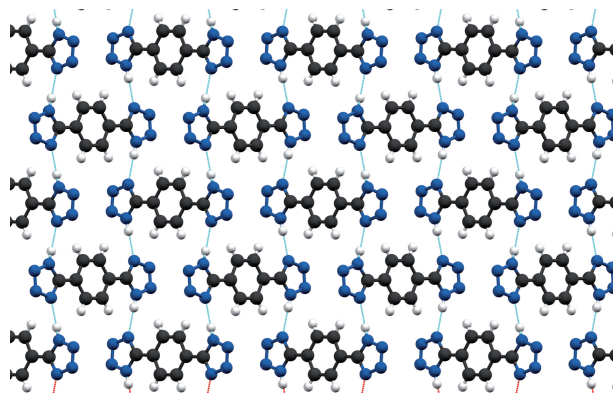


Fig. S1: Crystal structure of BTB (space group  $P2_1/c$ ), view down the crystallographic  $a$  axis.<sup>4</sup> Hydrogen bonds are depicted in turquoise.

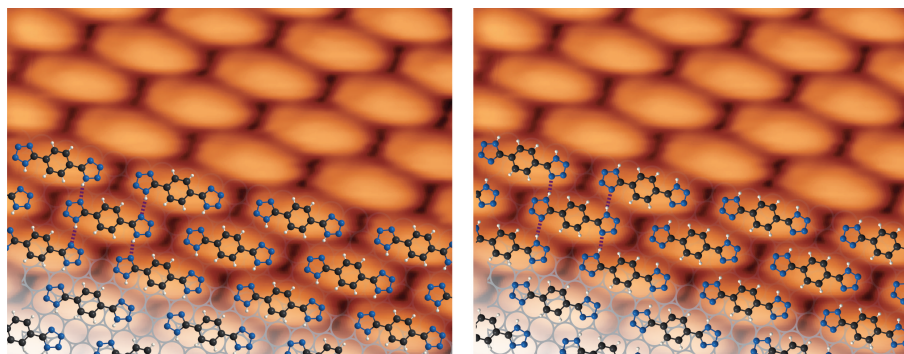


Fig. S2: STM image (1.25 V, 110 pA) of phase  $\alpha$ , overlaid with a possible model of BTB *cis* isomers. Black, blue and white spheres represent carbon, nitrogen and hydrogen, respectively. Although the *cis* isomer is achiral even in the 2D environment, the direction of the hydrogen bonding would impose organisational chirality in the 2D molecular islands. Purple dotted lines show the hydrogen bonding. Empty grey circles indicate the Ag(111) substrate atoms.

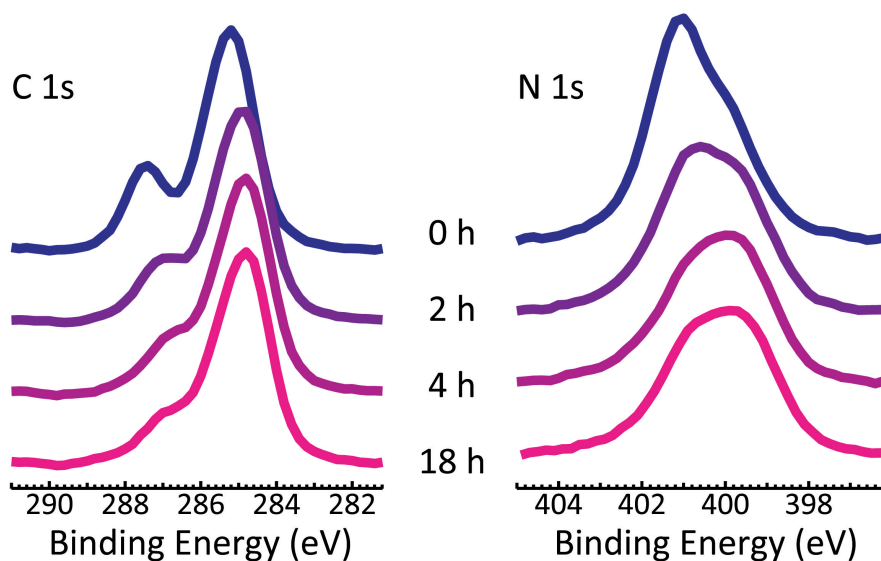


Fig. S3: XPS data of a monolayer BTB on Ag(111) evolving with time. From blue (directly after sublimation of BTB) to pink (18 h after sublimation).

Table S1: Relative intensities of C 1s and N 1s spectra presented in Fig. 3. Assignments A-E correspond to the A-E spectra in Fig. 3.

	C 1s (yellow)		C 1s (green)		C 1s (blue)	
	Binding energy [eV]	relative intensity	Binding energy [eV]	relative intensity	Binding energy [eV]	relative intensity
	C of the tetrazole (protonated)		C of the tetrazole (deprotonated)		C of the benzene	
A	287.3	24 %	286.2	1 %	285.2	75 %
B	287.0	14 %	286.0	12 %	284.8	74 %
C	286.8	12 %	285.8	15 %	284.6	73 %
D	287.1	20 %	286.0	10 %	285.2	72 %
E	286.9	13 %	286.0	15 %	284.9	74 %
	N 1s (blue)		N 1s (violet)			
	Binding energy [eV]	relative intensity	Binding energy [eV]	relative intensity		
A	401.3	70 %	400.0	30 %		
B	401.0	46 %	399.6	56 %		
C	401.0	26 %	399.4	74 %		
D	401.1	52 %	400.0	48 %		
E	400.8	40 %	399.7	60 %		

Table S2: Atomic ratios of C, N and Fe in the samples characterised by XPS, based on spectra with identical acquiring conditions and normalising with the photoionisation cross sections at the energy of the Mg  $K_{\alpha}$  line.<sup>5</sup>

	C 1s	N 1s	Fe 2p <sub>3/2</sub>
intensity (a.u.)	$1.32 \times 10^5$	$2.13 \times 10^5$	$3.87 \times 10^4$
atomic ratio	52 %	47 %	1 %

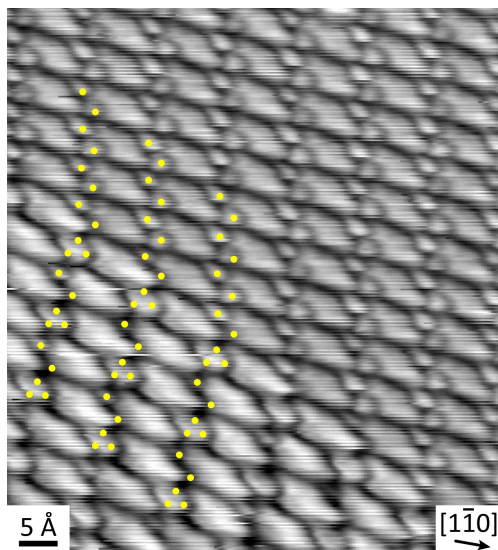


Fig. S4: STM image ( $-0.63$  V,  $90$  pA) of phases  $\beta$  and  $\gamma$ . Yellow dots indicate the proposed position for Ag adatoms.



Fig. S5: Schematic of transitions between phases  $\beta$  (unit cell in green) and  $\gamma$  (unit cell in yellow). Only transitions as shown in A (and symmetrically equivalent) have been observed. No transition of type B was detected, indicating the chiral recognition in the interface of these two phases.

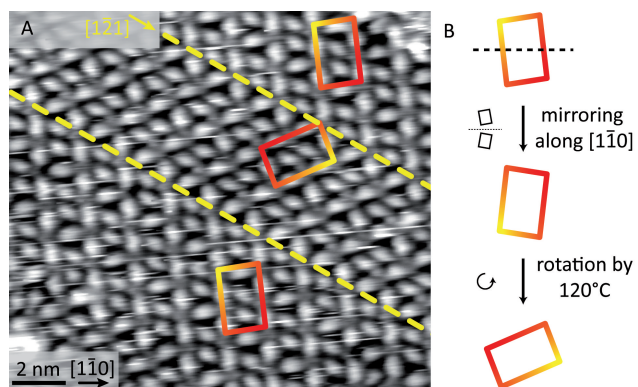


Fig. S6: (A) STM image (1.50 V, 60 pA) of phase  $\delta$ . Unit cells are displayed as colored rectangles. The seamless switching of symmetrically equivalent domains along the  $[1\bar{2}1]$  is accompanied by a chirality switch. (B) Schematic illustration of the chirality switch between the top/bottom part and the middle part of the image.

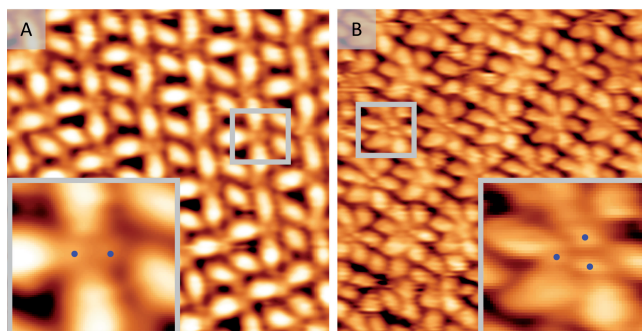


Fig. S7: STM images of phases  $\delta$  (A) and  $\epsilon$  (B). The insets show the marked parts magnified. Blue dots indicate the proposed positions for Fe adatoms.

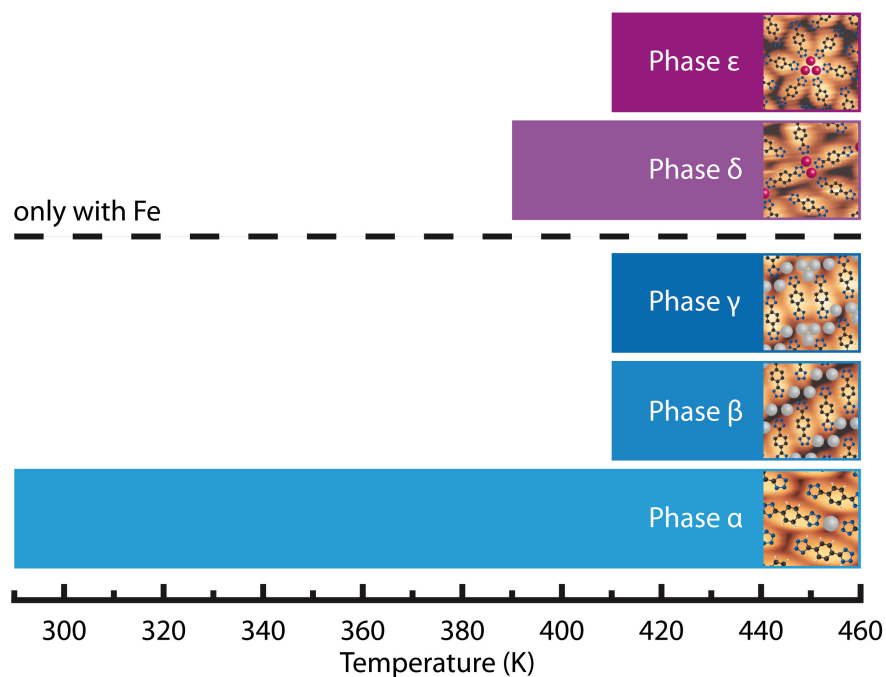


Fig. S8: Illustration of the thermally induced phase occurrence in dependence of the annealing temperature. Annealing temperatures higher than 460 K were not applied. Phases above the dotted line were only observed with Fe present on the surface. After annealing to 410 K all polymorphs coexist on the Ag(111) surface.

## References

- [1] L. Friedman and H. Shechter, *J. Org. Chem.*, 1961, 26, 2522–2524.
- [2] D. Vonlanthen, A. Rudnev, A. Mishchenko, A. Käslin, J. Rotzler, M. Neuburger, T. Wandlowski and M. Mayor, *Chem. Eur. J.*, 2011, 17, 7236–7250.
- [3] S. Vorona, T. Artamonova, Y. Zevatskii and L. Myznikov, *Synthesis*, 2014, 46, 781–786.
- [4] J.-H. Deng, X.-L. Yuan and G.-Q. Mei, *Inorg. Chem. Commun.*, 2010, 13, 1585–1589.
- [5] J. J. Yeh and I. Lindau, *At. Data Nucl. Data Tables*, 1985, 32, 1–155.